CrystEngComm

Accepted Manuscript

ROYAL SOCIETY OF CHEMISTRY

www.rsc.org/crystengcomm

Journal Name

RSCPublishing

ARTICLE

Generation of Luminescence in Biomineralized Zirconia by Zirconia-Binding Peptides

Cite this: DOI: 10.1039/xoxxoooooox

D. Rothenstein,[a] D. Shopova-Gospodinova,[a] G. Bakradze,[b] L.P.H. Jeurgens,[b,c] and J. Bill[a],

Received ooth January 2012,
Accepted ooth January 2012

DOI: 10.1039/xoxxoooooox

www.rsc.org/

Current materials research is inspired from biomineralization processes, where proteins control the formation of inorganic materials under soft reaction conditions. The implementation of biomineralization principles is a promising approach to generate tailored material properties for developing applications and devices. The results show the direct link between inorganic-binding peptides, biomineralization and the generation of new materials properties. Peptides which specifically bind to yttria-stabilized zirconia are selected by phage display and analyzed with regard to their amino acid composition. Based on these results the peptide 6-3-06 (SWNNMGWLPTFG) is selected for the peptide-assisted synthesis, generating biomineralized zirconia-based (BZO) material with photoluminescent properties. The material characterization by means of X-ray photoelectron spectroscopy reveals the incorporation of the peptide in the inorganic phase. More important this specific structure gives rise to photoluminescence (PL) in the blue wavelength region (~2.7 keV) at room temperature which is mainly attributed to states in the band gap introduced by organic-inorganic interfaces. This PL property is exclusive to the BZO whereas samples mineralized in the absence of the peptide did not show PL. The data clearly demonstrate that by biomineralization new material properties for technical materials can be generated. Importantly, this approach can be generalized for other inorganic materials.

Introduction

The main text of the article should go here with headings as appropriate. Zirconium dioxide (ZrO_2) is a highly interesting material applied in various devices like fuel cells,[1] thermal barrier coatings,[2] for catalysis,[3] and optical materials.[4] The wide scope of applications is based on its high abrasive, chemical, and thermal stability in addition to its semiconductive properties. To further engineer material properties, biomineralization approaches are favored for advanced materials generation. Biomineralization is the formation of bio/inorganic hybrid materials under ambient conditions controlled by organisms using biological molecules like proteins, or polysaccharides.[5] Natural biominerals often possess exceptional properties and multifunctionality. Such extraordinary properties are not present in the pure organic and inorganic materials but evolve from the combination of the two material classes. A prominent example is the mechanical stability of nacre.[6] Here, brittle aragonite (orthorhombic $CaCO_3$) platelets and soft proteins are arranged in a highly ordered brick wall formation which results in excellent toughness combined with stiffness, strength, and impact resistance.[7] The mechanical properties of nacre thereby outperform the properties of the constituent materials. Other examples are siliceous sponge spicules providing mechanical stability and light transmission.[8] Therefore, the transfer of biomineralization processes from nature to technical synthesis which allows the control of material properties would be highly beneficial for the development of novel materials for e.g. electronic and optical applications.

Several biomimetic approaches for the formation of ZrO_2 on organic templates have been reported in the literature: e.g. layer-by-layer deposited polycations and polyanions with a negatively charged surface layer[9, 10] and self-assembled monolayers.[11, 12] Furthermore, natural proteins have been applied for the synthesis of Zr-based materials. For example, it has been shown that silicatein, an enzyme isolated from sponges which catalyses the polycondensation of biosilica, also mediates the formation of Zr-based materials.[13] Other proteins, which are uncharacteristic for natural biomineralization processes, like lysozyme,[14] bovine serum albumin,[15] and gelatin[15] were also used for the mineralization of Zr-based materials. A step beyond such unspecific organic-inorganic interactions is the consideration of specific inorganic-binding peptides for the controlled biomineralization[16] which have not been applied for Zr-based materials so far. The phage display (PD) is a powerful technique to identify peptides from a random peptide library which specifically bind to inorganic materials. This method has been successfully applied for oxides

like ZnO,[17-21] SiO_2,[22] and TiO_2.[16] Furthermore, one peptide binding to yttria-stabilized zirconia (YSZ) which consists of 58 amino acids was identified by PD and applied in the surface functionalization of dental ceramics.[23]

This study shows the engineering of photoluminescence (PL) properties, as applied to biomineralized zirconia-based material (BZO), by the use of specific binding peptides. The PD technique was applied to select peptides from a random peptide library which bind specifically to single crystalline yttria-stabilized zirconia (YSZ) and powders of pure Y_2O_3 and ZrO_2. Enriched and depleted amino acids of the isolated peptides, which correspond to binding-favoring and -adverse components, have been deduced from the identified peptide pool. As an outcome of this investigation the YSZ-binding peptide 6-3-06, with the amino acid sequence SWNNMGWLPTFG, was selected to synthesize BZO. The elemental composition and the concentration ratio of O to Zr in the BZO phase were determined by X-ray photoelectron spectroscopy (XPS). The thus-produced BZO phase exhibited PL in the blue wavelength region (~2.7 eV), which was not present in the reference samples which were mineralized in the absence of the peptide. Therefore, by analogy with nacre, PL evolves from the interplay of the non-photoluminescent inorganic material with substrate specific peptides in BZO.

Experimental Section

Peptide screening

The phage display technique was applied to isolate ZrO_2-binding peptides from a random 12-mer peptide library (New England Biolabs, Inc). As a target substrate an (100)-oriented single crystal of yttria-stabilized (9.5 mol %) zirconia (YSZ) with cubic structure was used (CrysTec, Berlin, Germany). The peptide screening was conducted according to the procedures described elsewhere.[24] Briefly, the isolation of interacting peptides was conducted in 24 well plates (Sarstedt, Newton, USA). The substrate was equilibrated in Tris buffered saline (TBS), pH 7.5 supplemented with 0.1 % Tween 20 under light agitation for one hour at RT. M13 phages (1.5×10^{11} phages) expressing the peptide library were incubated with the target substrate in TBS, 0.1% Tween 20 (1 mL) for one hour at RT. Non-interacting phage clones were excluded by extensive washing with TBS, 0.5% Tween 20. The remaining peptide library was eluted with glycine elution buffer (1 mL, 0.2 M Glycine-HCl, pH 2.2, 1 mg/mL BSA). Afterwards, the solution was brought to a neutral pH value by the addition of Tris-HCl, (150 µL, 1 M, pH 9.1). For subsequent biopanning rounds and the analysis of the interacting peptides the eluted phage clones were amplified in *E. coli* ER2738 and purified by polyethylene glycol-8000 / sodium chloride (PEG/NaCl) precipitation. At least three biopanning rounds were carried out to enrich specifically binding peptides. Peptide sequences were deduced from DNA sequences from single phage clones.

Zeta potential measurement

The zeta potential of the epipolished YSZ(100) was measured with a SurPASS electrokinetic analyzer (Anton Paar, Graz, Austria). The substrates were cleaned according to Rabung et al.[25] and the zeta potential was determined in 75 mM NaCl solution using streaming current measurements.

Binding assay

The binding strength of individual ZrO_2-binding peptides was determined. Briefly, a phage clone expressing a ZrO_2-binding peptide sequence was amplified in *E. coli* ER2738 applying to standard methods. The individual phage clones were resuspended in TBS buffer (50 mM Tris pH 7.5; 150 mM NaCl). The phage titer was determined in three independent experiments.

For the binding assay, a defined quantity of phages or M13 wt phage, as reference, were bound to ZrO_2 in TBS at RT for 1 h. Unbound phages were excluded by 5 times washing the ZrO_2 with TBS supplemented with 0.5% Tween 20. Bound phages were finally eluted by lowering the pH value. The phage titer (number of bound phages) was determined using appropriate dilutions of the eluted phage solution. Only plates with a minimum of 50 plaque forming units (pfu) were included in the titer determination. The phage titer directly correlates with the binding strength of a single clone. The phage titers were normalized to wt phage titers (wt phage titer = 1).

Biomineralization of BZO

Chemicals were purchased from Sigma-Aldrich (Taufkirchen, Germany), peptides were synthesized at emc microcollections (Tübingen, Germany). Peptide solutions with 0.5 mg and 1.0 mg YSZ-binding peptide per 995 µL Tris-HCl (30 mM, pH 8.7) or sodium phosphate buffer (30 mM, pH 8.1) were prepared. Afterwards, Zr-nitrate solution (5 µL, 50 mM) was added and the solution was incubated at room temperature allowing the precipitation of particles. The particles were isolated by centrifugation for 20 min at 20817 x g. The precipitate was sonicated in ddH_2O and isolated by centrifugation as described above. In total, the samples were washed tree times to remove unspecific adsorbed peptides on the BZO particles. Finally the BZO particles were resuspended in ddH_2O (40 µL) for further analysis. A reference mineralization sample without the addition of a peptide was prepared following the same procedure as described above.

Scanning electron microscopy (SEM)

Mineralization products were immobilized on Si-wafers. To enhance the contrast, samples were sputtered with 0.5 nm platinum/palladium. SEM was performed with the Zeiss DSM 982 GEMINI scanning electron microscope at 3 kV.

PL measurement

To measure the photoluminescence the washed particles suspension (40 µL) were spotted on a cleaned silicon wafer and dried at 37°C for 24h. Silicon wafers (10 x 10 mm^2) were cleaned by consecutive sonication in ddH_2O and acetone / ethanol (1:1) with subsequent extensive washing. PL measurements were performed at room temperature. The emission spectrum (4.46 eV excitation) of ZrO_2 obtained in the presence and absence of the ZrO_2-binding peptide was recorded

with the spectrofluorometer Spex FluoroLog 3, Horiba Jobin Yvon, Germany.

XPS measurement

XPS spectra of the surfaces were recorded using a Thermo VG Thetaprobe system employing monochromatic Al Kα radiation (hν = 1486.68 eV). The valence-band (VB) spectra were recorded over the binding energy (BE) range from -5 to 35 eV with a step size 0.1 eV at a constant pass energy of 200 eV; the XPS spectra of the Zr 3d and O 1s regions were recorded over the BE range from 178 to 196 eV and from 526 to 543 eV with a step size of 0.05 eV at a constant pass energy of 100 eV and 60 eV respectively. The integral intensities of the Zr 3d and O 1s peaks were obtained using conventional XPS peak fitting routines, as implemented in the Avantage software (v.4.41), and employing a so-called smart´ shirley-type of background.

Results and discussion

Phage display

The peptide library was screened in three independent experiments for the binding to a cubic-structured YSZ(100) surface resulting in 30, 36 and 30 different peptide sequences, respectively. The isoelectric points (p*I*) of the isolated YSZ-binding peptides ranged from pH 3.5 to 12.5. Interestingly, the majority of peptides were charged under the screening conditions and only 1 % of peptides had a p*I* in the range between pH 7.0 and 7.9, reflecting no or only a small net charge (Figure 1).

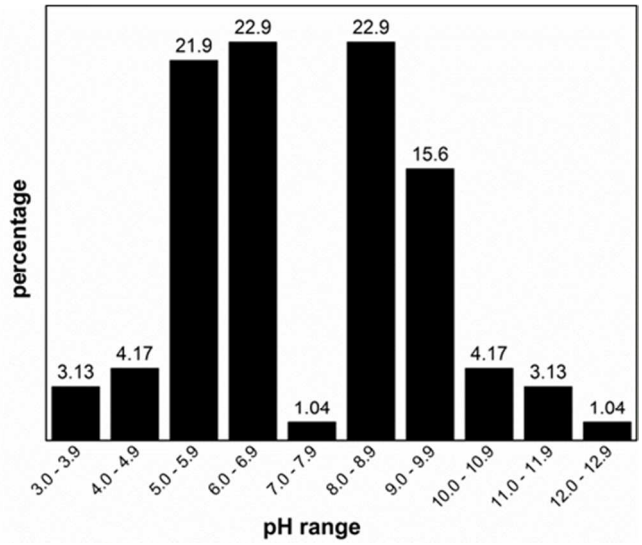

Figure 1. Isoelectric points (p*I*) of isolated YSZ-binding peptides. The percentages of peptides were plotted according to their calculated p*I*. The majority of peptides are charged under the screening conditions. Peptides with a zero net charge, having a p*I* around pH 7.5, were strongly underrepresented in the isolated peptide pool.

The zeta potential of the target YSZ(100) substrate was determined in the range between pH 5 and pH 10 at 75 mM NaCl (Figure 2). The target substrate was negatively charged over the whole investigated pH range with the isoelectric point (IEP) at around pH 5. At the pH value of the peptide screening (pH 7.5) the YSZ substrate had a negative charge of -30 to -35 mV. The isoelectric point for YSZ powder has been reported in the range of 6.6 and 7.2[26] with a surface charge between -5 to -12 mV at pH 7.5. Differences of the zeta potential for single crystalline and powder substrates were reported for other oxides (Al_2O_3, ZnO) as well.[15a, 19] The deviations were attributed to different charging mechanisms due to autoproteolysis of interfacial water molecules and water structuring, which resulted in the change of IEPs of single crystalline substrates.[27] Despite the differences in the IEP of single crystalline and powder target substrates, the amino acid frequencies of the isolated peptides from single crystalline and powder substrates showed major similarities (data not shown).

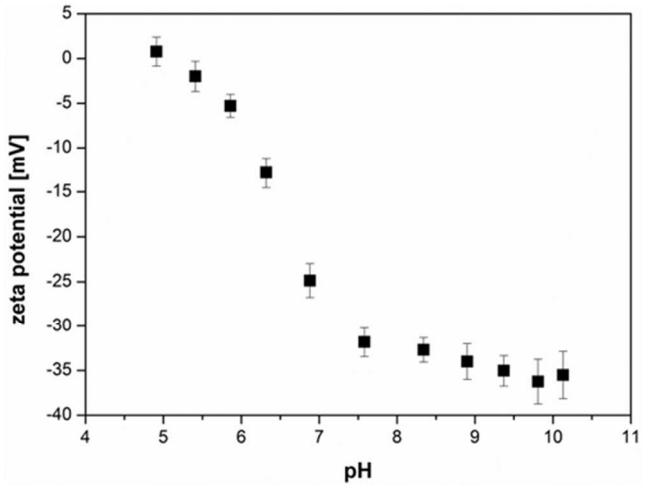

Figure 2. Zeta potential (ZP) of the YSZ (100) surface. The ZP was determined for the pH range between 5 and 10 in 75 mM NaCl solution in two independent experiments. The isoelectric point is at around pH 5. Under the conditions of peptide screening (pH 7.5) the substrate surface had a negative charge of -32 mV.

The amino acid residue frequencies of the YSZ-binding peptides in the isolated peptide pools were compared to those of the initial peptide library (Table 1). The quotient of a given amino acid frequency in the isolated peptide pool to that in the initial peptide library is indicative of its enrichment (*criterion*: quotient > 1.25) or depletion (*criterion*: quotient < 0.75) in the amino acid residue. The amino acid residues frequencies in the initial peptide library are manufacturer`s data based on sequencing individual clones. It followed that the categories of charged, small, and of aromatic amino acids exhibited substantial frequency changes, whereas the groups of hydrophobic and nucleophilic amino acids, as well as of amino acids with amid function, showed only very little changes. The following amino acid residues were enriched by more than 25 % in at least two out of three experiments; arginine (R), glycine (G), alanine (A), methionine (M), and tryptophan (W). While glutamic acid (E) and phenylalanine (F) were depleted by more than 25% compared to the initial library. The frequencies deviate between the independent experiments. For the majority of amino acid residues there is a clear classification, only lysine

(K) and tyrosine (Y) showed an ambiguous performance.

Table 1. Frequency of amino acid residues in YSZ-binding peptides. The frequencies are given as quotient of the amino acid frequency in the isolated peptide pool and in the initial peptide library. Enriched amino acid residues are highlighted dark grey, depleted amino acid residues are highlighted light grey.

Amino acid a)	basic			small		hydrophobic					acidic		amide		nucleophilic			aromatic		
	H	K	R	G	A	V	L	I	P	M	D	E	N	Q	S	T	C [b]	Y	F	W
Exp. 1	0.88	2.19	1.30	1.39	1.35	0.93	0.81	0.82	1.14	1.29	0.60	0.35	0.79	0.98	1.00	0.58	1.67	1.39	0.51	1.27
Exp. 2	1.10	0.58	1.25	1.96	1.16	1.07	1.02	0.54	0.97	1.34	1.07	0.22	1.21	0.59	0.95	0.96	0.46	0.84	1.05	1.37
Exp. 3	1.25	0.88	0.93	1.78	1.36	1.40	1.11	1.20	0.85	0.94	0.78	0.13	0.59	1.02	1.36	0.88	0.54	0.53	0.33	0.99
ZrO_2 powder	0.84	0.81	0.48	0.87	2.02	0.39	0.90	1.78	1.12	1.46	0.27	0.60	1.81	0.89	1.06	0.68	0.00	0.21	0.69	1.72
Y_2O_3 powder	1.07	0.30	1.61	2.26	0.84	0.65	1.36	0.00	0.83	1.94	2.10	0.27	0.55	0.82	0.84	0.83	5.04	0.70	0.76	1.91

a) Amino acids are indicated in one-letter code; b) The frequencies of cysteine residues were not included since cysteine interferes with the phage infection of bacteria and coat protein formation and therefore the values may not be based on binding.

The depletion of the negatively charged glutamic acid in the isolated peptides could be attributed to the electrostatic repulsion by the negatively charged YSZ(100) surface. However, aspartic acid, which is also negatively charged, showed no significant depletion in the isolated peptide pool. Hence, a simple peptide-inorganic binding model, based only on electrostatic attraction of charged particles, may be insufficient to explain the observed enrichments and depletions of amino acid residues in the isolated peptide pool. From the group of positively charged amino acid residues (histidine, lysine, and arginine), only arginine was enriched. Noteworthy, histidine did not show enhanced bonding affinity with YSZ, even though it is recognized as one of the most important natural interaction partners of divalent metal ions like Zn^{2+} and has been identified as strong interaction partner for inorganic ZnO.[17]

The peptide libraries were also screened for their binding properties with respect to pure ZrO_2 (without doping with Y) and pure Y_2O_3 powders (Table 1) (*note:* the hitherto mentioned results referred to single-crystalline YSZ). Methionine, glutamic acid and tryptophan exhibited similar binding properties to ZrO_2 and Y_2O_3 powders, which correlated well with their respective binding properties to YSZ. For several amino acid residues, only one type of powder (i.e. either pure ZrO_2 or pure Y_2O_3) showed similar frequency changes as compared to YSZ. For example, arginine and glycine were enriched solely in the Y_2O_3-binding peptides, whereas alanine was enriched and phenylalanine was depleted in the ZrO_2-binding peptides only. This suggests that certain amino acid residues discriminate between ZrO_2 and Y_2O_3. Summarizing: no preferred binding to either ZrO_2 or Y_2O_3 powder could be deduced for methionine, glutamic acid and tryptophan; alanine has a strong and phenylalanine a weak interaction with ZrO_2; arginine and glycine have a stronger interaction with Y_2O_3 than with ZrO_2.

Biomineralization and material characterization

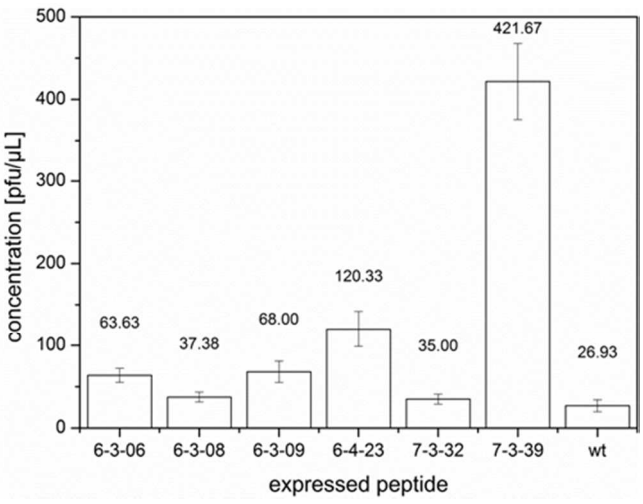

Figure 3. Relative binding of phage clones with ZrO_2. The binding of individual phage clones expressing selected ZrO_2-binding peptides for the binding to ZrO_2 was tested with a binding assay. Wild type (wt) phage was used as reference. Phage clones with a specific ZrO2-peptide showed a 1.3 to 15.6 fold increased binding to ZrO2. Although, the clone 6-3-06 only had a 2.5-fold increased binding strength compared to the wt phage, the peptide revealed the highest impact on the mineralization process.

On the basis of the combination of most distinctive ZrO_2-binding features, the peptide 6-3-06 (SWNNMGWLPTFG) was selected for further ZrO_2 biomineralization studies. This peptide displays three out of five amino acid residues, which were enriched in the YSZ-binding peptides. In addition, the peptide contains no glutamic acid, which was depleted in the isolated peptides. BZO was precipitated in the presence of the peptide from buffered Zr-nitrate solutions at pH values between 7.5 and 8.5. The YSZ-binding peptide 6-3-06 has a calculated p*I* of 5.52, which corresponds to a net charge of -0.1 to -0.8 mV in the biomineralization experiments. The binding-strength of the peptide was determined by a binding assay, where the peptide was linked to the phage clone (Figure 3). The values were referenced to the wild type (wt) phage, expressing no specific binding peptide. Although, the binding of the 6-3-06 harbouring

phage to ZrO_2 was moderate, peptide 6-3-06 showed the most significant impact on the properties of BZO. However, the peptide did not show a significant influence on the morphology of BZO (Figure 4). The BZO and the reference material, mineralized in the absence of peptide (data not shown), consisted of agglomerated nanoparticles of similar size.

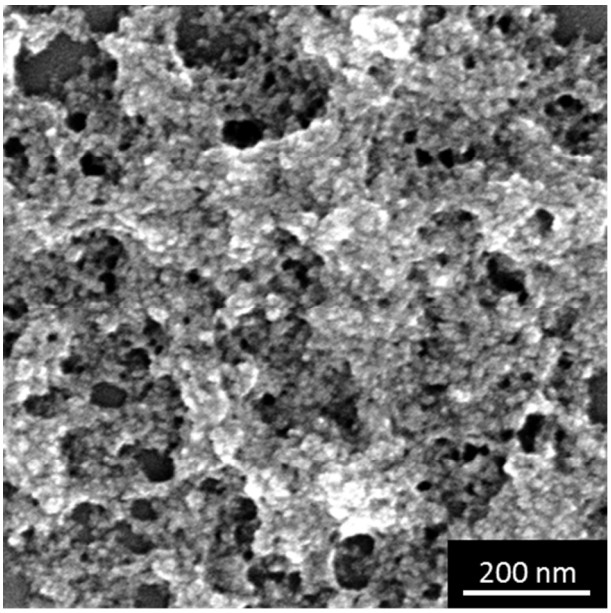

Figure 4. Scanning electron micrograph of biomineralized zirconia (BZO). BZO, mineralized in the presence of peptide 6-3-06, is a composite of agglomerated nanoparticles. The peptide does not significantly influence the morphology of BZO, since zirconia precipitated in the absence of the peptide exhibited the same structure (data not shown).

XPS was applied to determine the chemical constitutions of the BZO (as synthesized in the presence of the YSZ-binding peptide 6-3-06 on an Au-coated Si wafer) and the corresponding Zr-oxide reference (i.e. as synthesized under the same conditions in the absence of peptides) (Figure 5). The BZO and the Zr-oxide reference were both constituted of Zr, O, N and C (*note:* the detected Au signals in Figure 5 are originating from the Au-coated Si substrate). To exclude Tris buffer as the sole origin of nitrogen in the specimens, the biomineralization experiments were repeated in a phosphate buffered environment. In this case, nitrogen was detected only in the samples synthesized in the presence of the peptide 6-3-06 (with three different local chemical environments of N being resolved) (Figure 6). This implies that the detected N in the BZO phase originates from peptides, which have been incorporated during the biomineralization process. In addition, the average O/Zr-atomic-ratios of the BZO phase and the reference Zr-oxide were calculated from the integral areas of the resolved Zr $3d^3/_2$ and O 1s XPS peaks, according to the procedure described in Vinodh *et al.*[28] The thus determined O/Zr ratio of the biomineralized ZrO_2 phase equaled 3.3 before sputter cleaning (SC) and 2.2 after SC for 1 min with 1 kV Ar^+ ions, respectively. The ZrO_2 reference sample showed similar O/Zr ratios of 3.1 and 2.3 before and after SC, respectively. Hence both the biomineralized and reference Zr-oxide phases

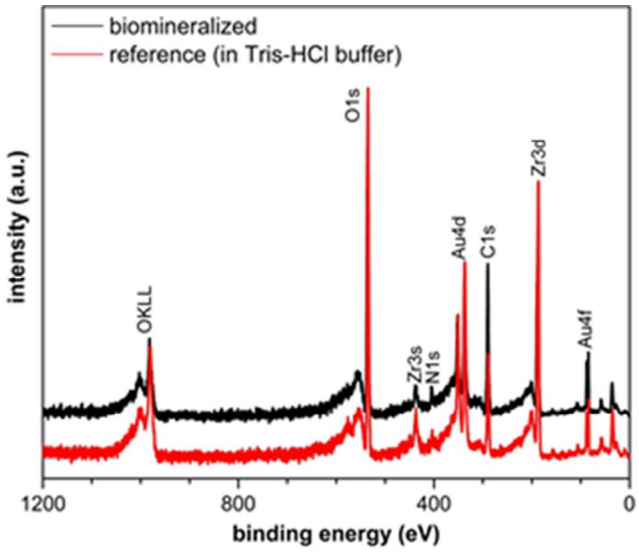

Figure 5. As-measured XPS spectra (after subtraction of a universal Tougaard background), as recorded from the biomineralized Zr-oxide and the corresponding Zr-oxide reference (both synthesized on an Au-coated Si wafer using a Tris-HCl buffered solution; see Experimental). The biomineralization was performed in the presence of the ZrO2-binding peptide 6-3-06. The reference was synthesized under the same conditions, but in the absence of peptides. The BE positions of the main core-level photoelectron lines and the O KLL Auger line are indicated.

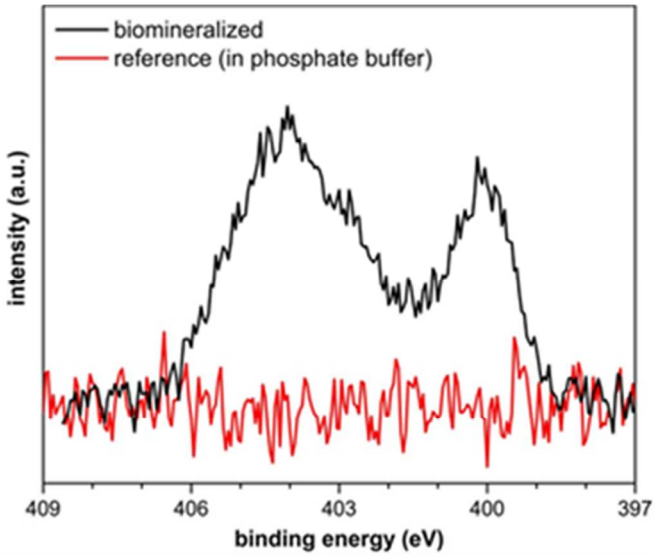

Figure 6. As-measured N 1s core-level XPS spectra (after subtraction of a Shirly background), as recorded from the BZO and the corresponding Zr-oxide reference (both synthesized on an Au-coated Si wafer using a phosphate buffered solution; see Experimental). The biomineralization was performed in the presence of the ZrO2-binding peptide 6-3-06. The reference was synthesized under the same conditions, but in the absence of peptides. The N in the biomineralized Zr-oxide phase originates from peptides, which have been incorporated during the biomineralization process.

are overall non-stoichiometric, in accordance with the observation of different valence (i.e. oxidation) states of Zr in the measured Zr 3d5 spectra of the biomineralized and reference samples (Figure 7). After removal of the top surface layers by gentle SC, the averaged O/Zr-ratio (of 2.2±0.1) approaches that of stoichiometric ZrO_2 (*note:* the averaged

O/Zr-ratio of 3.2±0.1 before SC (for both specimens) is much higher than the corresponding stoichiometric of ZrO_2). This suggests that the chemical constitution of the reaction product, as precipitated from the solution and transferred onto the Si-gold substrate surface, is subsequently transformed into a bulk oxide phase of different composition. Furthermore, the incorporated peptide in the BZO sample slightly contributes to the oxygen content in the sample. Finally, as evidenced from the featureless shape of the Upper Valence Band (UVB) region (not shown here), as resolved from the measured XPS valence band spectra of the BZO phase (according to the procedure described in Ref.[29]), the BZO phase and the reference sample are both amorphous and highly defective.

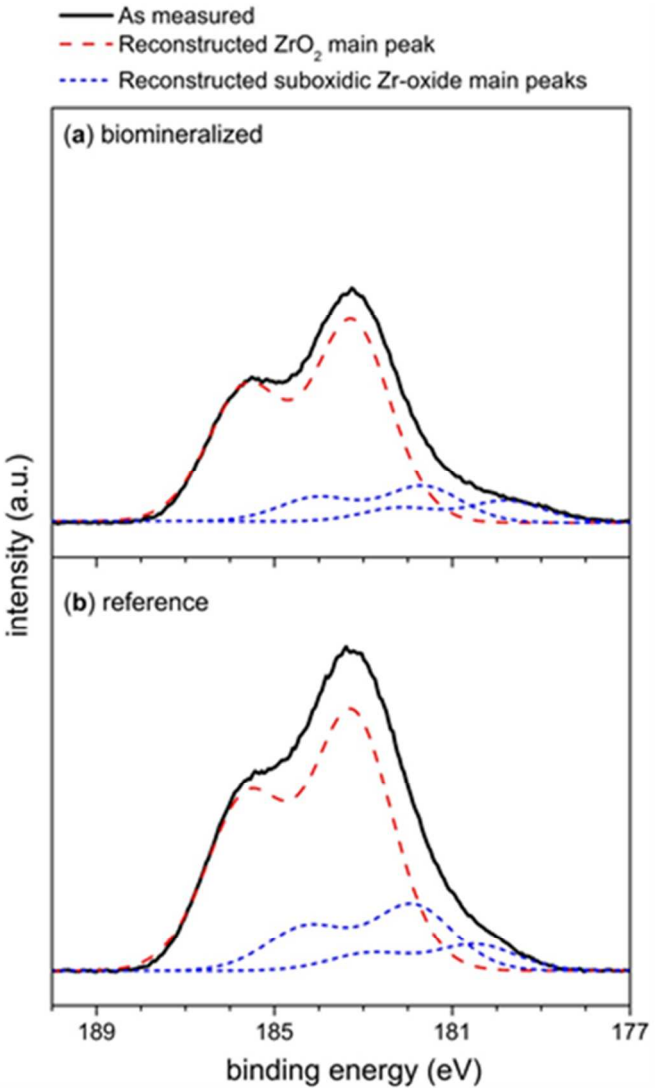

Figure 7. As-measured and reconstructed Zr 3d XPS spectra (after Shirley background subtraction), as recorded from the BZO and the corresponding Zr-oxide reference. For details, see caption of Figure 4.

Next the PL properties of the BZO and the reference samples were measured (Figure 8). The BZO exhibits a PL band around 2.7 eV; its intensity correlates with the concentration of peptide used in the mineralization reaction, i.e. a higher peptide concentration yields a stronger PL intensity. The reference Zr-

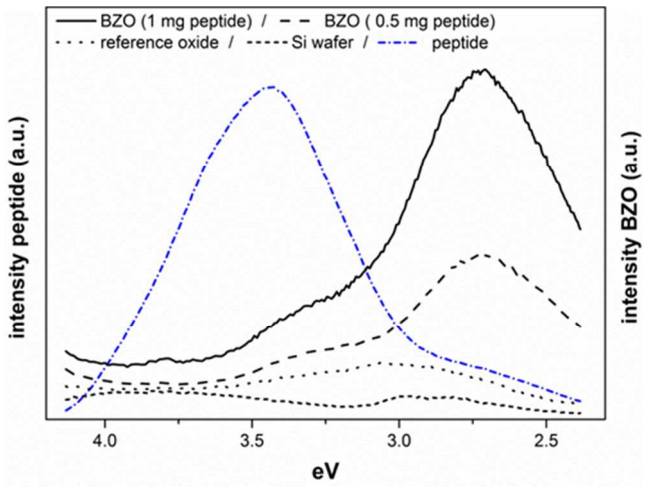

Figure 8. Photoluminescence (PL) spectra of biomineralized Zr-oxide (BZO) and the peptide 6-3-06 only. The emission spectrum (4.5 eV excitation) of the biomineralized Zr-oxide obtained in the presence of the ZrO_2-binding peptide exhibit a peak at around 2.7 eV, which can be attributed to structural defects induced by the incorporation of the ZrO_2-binding peptides. The peak intensity was correlated with the peptide concentration in the biomineralization experiment. The reference Zr-oxide mineralized in the absence of the peptide did not show a considerable signal. For comparison, the emission band of the ZrO_2-binding peptide only was determined. The emission band peaks around 3.5 eV and corresponds to the PL band of the aromatic tyrosine residues. The PL band of the peptide and the BZO is different

oxide sample, as mineralized in the absence of YSZ-binding peptides, does not show any pronounced emission in the studied wavelength range. The emission spectrum of the inorganic-binding peptide also does not exhibit any PL intensity maximum around 2.7 eV but shows a maximum around 3.5 eV which is attributed to the fluorescence of tryptophan residues. Hence, the unique intensity maximum around 2.7 eV in the PL band of BZO originates from the incorporation of the peptides in BZO. It is therefore suggested that the organic-inorganic interface between the incorporated peptides and the oxide produce specific states in the band gap of the BZO materials which give rise to the observed PL intensity around 2.7 eV. It is emphasized that, although the reference oxide (as produced in the absence of the peptide) is also amorphous and highly defective, it does not exhibit a PL intensity maximum around 2.7 eV.

Despite considerable research efforts on the optical properties of zirconia, there is no generally accepted PL mechanism so far. This is partly due to a fact that the luminescent properties of zirconia seem to be strongly dependent on the preparation method.[30] Two kinds of luminescence in zirconia are known, (i) luminescence of self-trapped excitons peaking around 4.3 eV,[31] which is typically observed at low temperatures, and (ii) intrinsic-defect-related luminescence covering a broad spectral range within 1.5-3.5 eV (e.g. F^{+32} or other electron trapping centers[33]). Recently, Grigorjeva *et al.*[34] observed a wide featureless PL band peaking around 2.8 nm recorded from ZrO_2 single crystals, nanocrystals and ceramics. The authors argued that the wide PL band in the emission spectra of ZrO_2 arises due to the zirconium-oxygen complexes, which are distorted

around an intrinsic defect (e.g. an oxygen vacancy). However, though the reference Zr-oxide, as produced in the absence of the peptide in our study, is highly defective and amorphous (see the discussion of the XPS data above) it does not exhibit any considerable PL intensity. Therefore, it is suggested that the PL band peaking around 2.7 eV originates from the luminescence centers, which are introduced exclusively by incorporation of the ZrO_2-binding peptide molecules into the bulk biomineralized Zr-oxide. As the PL band observed in Figure 8 is wide, it cannot be excluded that the emission is caused by a number of different luminescence centers.

This study shows that optical properties of biomineralized materials can be generated by the interaction of specific peptides with corresponding inorganic materials. Further research on BZO will target at controlling both the material properties and the morphology by genetic engineered biotemplates for nanotechnology applications.

Conclusion

In summary, peptides binding to YSZ were identified from a random peptide library applying the PD method. Amino acid residues which account for the support or impediment of binding were identified. Although, a unique binding motif could not be determined on the basis of the conserved amino acid residues, prerequisites for zirconia-binding were established. The lack of YSZ-binding peptides with a no net charge suggests that the organic-inorganic binding results among other factors from electrostatic interactions.

Based on a combination of distinctive binding features, the peptide 6-3-06 was selected for BZO mineralization. The chemical constitution of the BZO is amorphous and non-stoichiometric and exhibits a broad photoluminescence band around 2.7 eV at room temperature, which is more pronounced at higher peptide concentrations in the biomineralization process. This band is attributed to states in the band gap of BZO, which are most likely introduced by incorporation of the peptide into the bulk amorphous oxide phase during the deposition process.

Acknowledgements

The authors are grateful to Mrs. M. Wieland for XPS measurements, Mrs. S. Scherb for PL sample preparation and measurement, Dr. P. Atanasova for providing the AFM picture of M13 phages, and the MPI for Intelligent Systems (formerly MPI for Metals Research). The financial support from the German Research Foundation (DFG, grant RO 3965/1-1) is greatly acknowledged.

Notes and references

[a]Institute for Materials Science, University of Stuttgart, Heisenbergstraße 3, 70569 Stuttgart, Germany.

[b] Max Planck Institute for Intelligent Systems (formerly MPI for Metals Research), Dept. Mittemeijer, Heisenbergstrasse 3, 70569 Stuttgart, Germany

[c] Present address Empa, Swiss Federal Laboratories for Materials Science and Technology, Ueberlandstrasse 129, 8600 Duebendorf, Switzerland.

1. R. M. Ormerod, *Chem. Soc. Rev.*, 2003, **32**, 17-28.
2. C. G. Levi, *Curr. Opin. Solid State Mater. Sci.*, 2004, **8**, 77-91.
3. F. C. Jentoft, A. Hahn, J. Kröhnert, G. Lorenz, R. E. Jentoft, T. Ressler, U. Wild, R. Schlögl, C. Häßner and K. Köhler, *J. Catal.*, 2004, **224**, 124-137.
4. R. Hahn, S. Berger and P. Schmuki, *J. Solid State Electrochem.*, 2010, **14**, 285-288.
5. E. Bäuerlein, P. Behrens and M. Epple, *Handbook of biomineralization*, Wiley-VCH, Weinheim, 2007.
6. M. A. Meyers, P. Y. Chen, A. Y. M. Lin and Y. Seki, *Prog. Mater Sci.*, 2008, **53**, 1-206.
7. S. Kamat, X. Su, R. Ballarini and A. H. Heuer, *Nature*, 2000, **405**, 1036-1040.
8. W. E. G. Müller, M. Kasueske, X. Wang, H. C. Schröder, Y. Wang, D. Pisignano and M. Wiens, *Cellular and Molecular Life Sciences*, 2009, **66**, 537-552.
9. I. Zlotnikov, I. Gotman and E. Y. Gutmanas, *Appl. Surf. Sci.*, 2008, **255**, 3447-3453.
10. M. R. De Guire, T. P. Niesen, S. Supothina, J. Wolff, J. Bill, C. N. Sukenik, F. Aldinger, A. H. Heuer and M. Ruhle, *Zeitschrift für Metallkunde*, 1998, **89**, 758-766.
11. M. Agarwal, M. R. De Guire and A. H. Heuer, *J. Am. Ceram. Soc.*, 1997, **80**, 2967-2981.
12. T. Salami, Q. Yang, K. Chitre, S. Zarembo, J. Cho and S. Oliver, *J. Electron. Mater.*, 2005, **34**, 534-540.
13. M. N. Tahir, P. Theato, W. E. G. Müller, H. C. Schröder, A. Borejko, S. Faiss, A. Janshoff, J. Huth and W. Tremel, *Chem. Commun.*, 2005, 5533-5535.
14. Y. Jiang, D. Yang, L. Zhang, Y. Jiang, Y. Zhang, J. Li and Z. Jiang, *Industrial & Engineering Chemistry Research*, 2008, **47**, 1876-1882.
15. H. J. Ji, X. H. Liu, X. Wang, X. D. Wu, X. J. Yang and L. D. Lu, *Colloids and Surfaces a-Physicochemical and Engineering Aspects*, 2009, **346**, 1-4.
16. M. B. Dickerson, K. H. Sandhage and R. R. Naik, *Chem. Rev.*, 2008, **108**, 4935-4978.
17. D. Rothenstein, B. Claasen, B. Omiecienski, P. Lammel and J. Bill, *J. Am. Chem. Soc.*, 2012, **134**, 12547-12556.
18. C. K. Thai, H. X. Dai, M. S. R. Sastry, M. Sarikaya, D. T. Schwartz and F. Baneyx, *Biotechnol. Bioeng.*, 2004, **87**, 129-137.
19. K. Kjaergaard, J. K. Sorensen, M. A. Schembri and P. Klemm, *Applied and Environmental Microbiology*, 2000, **66**, 10-14.
20. M. M. Tomczak, M. K. Gupta, L. F. Drummy, S. M. Rozenzhak and R. R. Naik, *Acta Biomaterialia*, 2009, **5**, 876-882.
21. M. Umetsu, M. Mizuta, K. Tsumoto, S. Ohara, S. Takami, H. Watanabe, I. Kumagai and T. Adschiri, *Adv. Mater.*, 2005, **17**, 2571-2575.
22. R. R. Naik, L. L. Brott, S. J. Clarson and M. O. Stone, *J. Nanosci. Nanotechnol.*, 2002, **2**, 95-100.

23. K. Hashimoto, M. Yoshinari, K. Matsuzaka, K. Shiba and T. Inoue, *Dental Materials Journal*, 2011, **30**, 935-940.
24. D. Rothenstein, J. Baier, T. Schreiber, V. Barucha and J. Bill, *Aquat Biosyst*, 2012, **8**, 31.
25. T. Rabung, D. Schild, H. Geckeis, R. Klenze and T. Fanghanel, *J. Phys. Chem. B*, 2004, **108**, 17160-17165.
26. W.-C. J. Wei, S.-C. Wang and F.-Y. Ho, *J. Am. Ceram. Soc.*, 1999, **82**, 3385-3392.
27. J. Lützenkirchen, R. Zimmermann, T. Preocanin, A. Filby, T. Kupcik, D. Kuttner, A. Abdelmonem, D. Schild, T. Rabung, M. Plaschke, F. Brandenstein, C. Werner and H. Geckeis, *Adv. Colloid Interface Sci.*, 2010, **157**, 61-74.
28. M. S. Vinodh and L. P. H. Jeurgens, *Surf. Interface Anal.*, 2004, **36**, 1629-1636.
29. G. Bakradze, L. P. H. Jeurgens and E. J. Mittemeijer, *J Phys Chem C*, 2011, **115**, 19841-19848.
30. C. Lin, C. Zhang and J. Lin, *The Journal of Physical Chemistry C*, 2007, **111**, 3300-3307.
31. M. Kirm, J. Aarik, M. Jürgens and I. Sildos, *Nucl Instrum Meth A*, 2005, **537**, 251-255.
32. N. G. Petrik, D. P. Taylor and T. M. Orlando, *J. Appl. Phys.*, 1999, **85**, 6770-6776.
33. S.-C. Chang and C.-S. Su, *Radiat. Prot. Dosim.*, 1993, **47**, 169-172.
34. L. Grigorjeva, D. Millers, A. Kalinko, V. Pankratov and K. Smits, *J. Eur. Ceram. Soc.*, 2009, **29**, 255-259.

